Early loss of cardiac function in acute myocardial infarction is associated with redox imbalance

Angela Maria Vicente Tavares PhD[1], Alex Sander da Rosa Araujo PhD[1], Susana Llesuy PhD[2], Neelam Khaper PhD[3], Luis Eduardo Rohde MD[4], Nadine Clausell MD[4], Adriane Belló-Klein PhD[1]

AMV Tavares, AS da Rosa Araujo, S Llesuy, et al. Early loss of cardiac function in acute myocardial infarction is associated with redox imbalance. Exp Clin Cardiol 2012;17(4):263-267.

BACKGROUND: The loss of viable myocardium subsequent to myocardial infarction (MI) impairs cardiac function, and oxidative stress is considered to be critical in this process.
OBJECTIVES: To assess cardiac function and correlate it with oxidative stress and antioxidant levels in cardiac tissue at 48 h post-MI.
METHODS: Adult male Wistar rats (n=6 per group) with a mean (± SD) weight of 229±24 g were randomly assigned to either an infarcted group or a control group. MI was induced by occlusion of the left coronary artery. Cardiac function was evaluated by measuring left ventricular (LV) ejection fraction, LV fractional shortening, cardiac output, myocardial performance index and the peak early diastolic velocity/peak atrial velocity ratio using echocardiography. The myocardial oxidative stress profile was assessed by measuring the reduced glutathione/oxidized glutathione ratio, H_2O_2 levels, peroxiredoxin-6 protein levels and activity levels of superoxide dismutase, catalase and glutathione peroxidase. Lipid peroxidation was quantified using chemiluminescence, and protein oxidation was determined by measuring protein carbonyl levels.
RESULTS: LV ejection fraction and LV fractional shortening were lower in the infarcted group compared with the sham group, whereas the peak early diastolic velocity/peak atrial velocity ratio and myocardial performance index were significantly increased, indicating systolic dysfunction. Lipid peroxidation, protein carbonyls and superoxide dismutase and catalase activity levels did not differ between the groups. Peroxyredoxin-6 levels were increased in the infarcted group, while H_2O_2 levels were reduced. The reduced glutathione/oxidized glutathione ratio and the glutathione peroxidase activity were reduced in the infarcted group compared with control.
DISCUSSION AND CONCLUSION: These data suggest that MI-induced cardiac dysfunction and impaired redox balance may be associated with the activation of counter-regulatory responses to maintain reduced H_2O_2 concentrations and, thereby, prevent further oxidative damage at this early time point.

Key Words: *Acute myocardial infarction; Cardiac function; Redox imbalance*

An adequate oxygen supply is necessary to sustain cell viability and basal metabolism. The production of reactive oxygen species (ROS) occurs as a result of aerobic metabolism, and ROS participate in many cellular functions including the cell signalling process (1). ROS are oxygen-derived chemical species that include free radicals, such as superoxide anion ($O_2^{\cdot -}$) and hydroxyl radical ($OH^{\cdot}$), and nonradicals such as H_2O_2 (2).

Excessive ROS production may occur when the oxygen supply is deficient (eg, during ischemia) (3). In this situation, irreversible cellular damage may occur because ROS can oxidize membrane phospholipids, proteins and DNA. Thus, ROS are implicated in the pathogenesis of myocardial infarction (MI) (4). Subsequent to MI, the heart undergoes a remodelling process that leads to hypertrophy of surviving myocytes and hyperplasia of nonmyocytes (5). These responses initially serve as an adaptive process, but are often accompanied by cardiac decompensation and heart failure (6). H_2O_2 has a central role in this process and, depending on its concentration, may drive intracellular signalling to adaptive or maladaptive pathways (7). At low levels, H_2O_2 can stimulate cardiac cell growth; however, in high concentrations it may cause cardiomyocyte apoptosis (8). Thus, the modulation of H_2O_2 concentration is important in this context and is accomplished by intracellular antioxidant systems.

The toxic effects of ROS can be abrogated by enzymatic as well as nonenzymatic antioxidants (9). For instance, H_2O_2 is metabolized by enzymes such as catalase (CAT), glutathione peroxidase (GPx) and peroxiredoxin (Prx). CAT is an enzyme specific to H_2O_2 detoxification and is active when H_2O_2 levels are in the micromolar range (10). However, its activity is very low in heart tissue, where GPx has a more relevant role (9). GPx catalyzes the removal of H_2O_2 and hydroperoxides through the oxidation of reduced glutathione (GSH), producing oxidized glutathione (GSSG) (11). The GSH/GSSG ratio is a strong indicator of the cellular redox state. Prx also possesses peroxide scavenging activities and is expressed in all vital organs, including the heart (12,13). Prx is a superfamily of peroxidases that uses thioredoxin and GSH as electron donors in the detoxification of peroxides (14,15). Certain Prx isoforms have been demonstrated to be downregulated in patients with cardiomyopathy (16).

It is clear from the literature cited that deficient antioxidant adaptations to the maintenance of steady H_2O_2 concentrations and, therefore, the redox state are crucial to the development of heart failure subsequent to MI. Although many studies have explored the mechanisms involved in ventricular remodelling, relatively little is known regarding the role of antioxidant changes in cardiac cells postischemia, during the very early stages of heart failure.

Thus, the aim of the present study was to evaluate cardiac function using echocardiography and correlate it with oxidative stress and antioxidant reserve in cardiac tissue at 48 h postexperimental MI.

METHODS

Animals and groups

Male Wistar rats, eight weeks of age, weighing 229±24 g, were used in the present study (n=6 per group). Animals were maintained in compliance with the Principles of Laboratory Animal Care, formulated by the National Institutes of Health (publication number 96-23, revised 1996).

The present study was approved by the ethics and research committee of Hospital de Clínicas de Porto Alegre (Porto Alegre, Brazil). Animals were randomly assigned to two groups: a control (sham) group, and an infarcted group that underwent a surgical procedure to induce MI. All animals were housed in a temperature-controlled animal facility with a 12 h light/12 h dark cycle and were fed ad libitum with rat chow.

[1]*Cardiovascular Physiology Laboratory, Basic Sciences Institute, Universidade Federal do Rio Grande do Sul, Porto Alegre, Brazil;* [2]*Universidad de Buenos Aires, Buenos Aires, Argentina;* [3]*Medical Sciences Division, Northern Ontario School of Medicine, Lakehead University, Thunder Bay, Ontario;* [4]*Cardiovascular Research Laboratory Research Centre, Hospital de Clínicas de Porto Alegre, Brazil*
Correspondence: Adriane Belló Klein, Cardiovascular Physiology Laboratory, Basic Sciences Institute, Universidade Federal do Rio Grande do Sul, Porto Alegre, Brazil. Telephone 55-51-3-308-3621, fax 55-51-3-308-3621, e-mail belklein@ufrgs.br

MI surgery

MI was induced according to a previously described procedure (17) and adapted in the authors' laboratory. Briefly, animals were placed in the dorsal decubitus position and anesthetized with xylazine (0.67 mg/kg administered intraperitoneally) and ketamine (0.33 mg/kg administered intraperitoneally). Following orotracheal intubation, animals were submitted to mechanical ventilation (Harvard ventilator model 683, Harvard Apparatus, USA). A left intercostal thoracotomy was performed without exteriorization of the heart. The left anterior descending coronary artery was occluded with a 6-0 mononylon suture. The thoracic cavity was closed with a 5-0 mononylon suture (18). The sham group was subjected to the same surgical procedure but the coronary artery ligation was not performed.

Echocardiogram

All animals underwent echocardiography assessment before surgical interventions (baseline) and 48 h following the surgical procedures. Transthoracic echocardiography was performed using the EnVisor Philips system (Andover, USA) with a 12-4 MHz transducer set at 2 cm depth with fundamental and harmonic imaging. All the measurements and calculations were performed in accordance with the American Society of Echocardiography.

Left ventricular (LV) dimensions: The LV end-diastolic and end-systolic transverse areas (cm^2) were obtained by tracing the endocardial border at three levels: basal (at the tip of the mitral valve leaflets); middle (at the papillary muscle level); and apical (distal from the papillary muscle but before the final curve cavity) (19).

Infarct size (IS): In each echocardiographic transverse plane, the arc corresponding to the infarcted segments (the akinetic and/or hypokinetic region) and the total endocardial perimeter were measured at end-diastole. IS was expressed as a percentage and was estimated using the following equation (20):

$$IS = (\text{akinetic and/or hypokinetic region/endocardial perimeter}) \times 100$$

LV systolic function: LV ejection fraction (LVEF) was calculated using the following equation:

$$LVEF = (\text{end-diastolic volume} - \text{end-systolic volume/end-diastolic volume}) \times 100$$

LVEF was expressed as a percentage; end-diastolic and end-systolic volumes were calculated using Simpson's rule (21). Cardiac output (CO) was calculated using the following equation:

$$CO = \text{end-systolic volume} \times \text{heart rate (HR)}$$

LV fractional shortening (LVFS) was calculated using the following equation (22,23):

$$LVFS = \text{diastolic diameter} - \text{systolic diameter/diastolic diameter} \times 100.$$

LV diastolic function: LV diastolic function was assessed by peak early diastolic velocity (E) and peak atrial velocity (A) ratio as a measure of mitral diastolic flow.

Myocardial performance index (MPI): MPI was calculated by measuring LV ejection time (ET) and mitral flow time with Doppler imaging by using the following equation (24):

$$MPI = (\text{mitral flow time} - ET)/ET$$

Data were recorded on a compact disc for later review and offline analysis. Subsequent to echocardiography assessment, the animals were euthanized by cervical dislocation.

Tissue preparation

After animals were euthanized, the hearts were rapidly excised, weighed and subsequently homogenized in 1.15% w/v KCl and phenylmethylsulfonyl fluoride (PMSF) 20 mM using a tissue homogenizer. The resulting suspension was centrifuged at 600 *g* for 10 min at 4°C to remove nuclei and cell debris (25) and the supernatant was used for oxidative stress measurements. The left ventricle was removed and frozen at −80°C immediately after euthanasia for the measurement of glutathione as well as for Western blot analysis.

Determination of lipid peroxidation using tert-butyl-hydroperoxide-initiated chemiluminescence

Chemiluminescence was measured in a liquid scintillation counter set to the out-of-coincidence mode (Rack Beta liquid scintillation spectrometer 1215, LKB Produkter AB, Sweden). Homogenates were placed in low-potassium vials at a protein concentration of 0.5 mg/mL to 1.0 mg/mL in a reaction medium consisting of 120 mM KCl and 30 mM phosphate buffer (pH 7.4). Measurements were initiated by the addition of 3 mM tert-butyl hydroperoxide and data were expressed as counts per s (cps)/mg protein (26).

Determination of protein oxidative damage using the protein carbonyl assay

Tissue samples were incubated with 2,4-dinitrophenylhydrazine (DNPH 10 mM) in a 2.5 M HCl solution for 1 h at room temperature in the dark. Samples were vortexed every 15 min. Subsequently, a 20% trichloroacetic acid (w/v) solution was added and the solution was incubated on ice for 10 min and centrifuged for 5 min at 1000 *g* to collect protein precipitates. An additional wash was performed with 10% trichloroacetic acid (w/v). The pellet was washed three times with ethanolethyl acetate (1:1) (v/v). The final precipitates were dissolved in 6 M guanidine hydrochloride solution and incubated for 10 min at 37°C, and the absorbance was measured at 360 nm (27).

Determination of H_2O_2 levels

The assay was based on the horseradish peroxidase-mediated oxidation of phenol red by H_2O_2. Slices of the left ventricle were incubated for 30 min at 37°C in 10 mM phosphate buffer (140 mM NaCl and 5 mM dextrose). Supernatants were transferred to tubes with 0.28 mM phenol red and 8.5 U/mL horseradish peroxidase. After a 5 min incubation, 1 M NaOH was added and the absorbance was measured at 610 nm. The steady-state concentration of H_2O_2 was expressed in nmol H_2O_2/g tissue (28).

Western blot analysis

Tissue homogenization, electrophoresis and protein transference were performed as described elsewhere (29,30). Membranes were processed for immunodetection using rabbit anti-Prx-6 (25 kDa) as the primary antibody (Santa Cruz Biotechnology, USA).

The bound primary antibodies were detected using goat anti-rabbit horseradish peroxidase-conjugated secondary antibody (Santa Cruz Biotechnology, USA), and the membrane was developed using chemiluminescence. Signal intensities were quantitatively analyzed using an image densitometer (ImageMaster DS CI, Amersham Biosciences Europe, Italy). Molecular weights of the bands were determined by referring to a standard molecular weight marker (RPN 800 rainbow full range, Bio-Rad Laboratories Inc, USA). The Ponceau red method was used to normalize the signal intensities of the bands from each membrane (31).

Determination of antioxidant enzyme activities

The quantification of SOD activity, expressed as U/mg protein, was based on the inhibition of the reaction between $O_2^{\cdot -}$ and pyrogallol (32). CAT activity was determined by measuring the decrease in H_2O_2 absorbance at 240 nm. CAT activity was expressed as µmol H_2O_2 reduced/min/mg protein (10). GPx activity was expressed as nmol peroxide/hydroperoxide reduced/min/mg protein and was based on the consumption of NADPH at 480 nm (33).

Determination of total glutathione and GSSG concentration

To determine GSSG and total glutathione concentration, tissue was homogenized in 2 M perchloric acid and centrifuged at 1000 *g* for 10 min, and 2 M KOH was added to the supernatant. The reaction medium

TABLE 1
Echocardiographic parameters in sham and infarcted groups

Parameters	Groups		P
	Sham	Infarcted	
Systolic diameter, cm	0.27±0.08	0.50±0.03	0.0001
Diastolic diameter, cm	0.64±0.08	0.72±0.05	ns
LVEF, %	77±7	51±5	0.0002
LVFS, %	61±9	30±4	0.0001
Cardiac output, mL/min	87±17	72±28	ns
E, m/s	1.24±0.11	1.43±0.24	ns
A, m/s	0.70±0.13	0.45±0.09	0.0038
E/A ratio	1.78±0.23	3.24±0.84	0.0048
Myocardial performance index	0.24±0.06	0.59±0.14	0.0009

Data are expressed as mean ± SD unless otherwise indicated. A Peak atrial velocity; E Peak early diastolic velocity; LVEF Left ventricular ejection fraction; LVFS Left ventricular fractional shortening; ns Not statistically significant; P values were calculated using Student's t *test*

contained 100 mM phosphate buffer (pH 7.2), 2 mM NADPH, 0.2 U/mL glutathione reductase and 70 µM 5,5'-dithiobis(2-nitrobenzoic acid). To determine the GSSG concentration, the supernatant was neutralized with 2 M KOH and inhibited by the addition of 5 µM N-ethylmaleimide. Absorbance was read at 420 nm (34). GSH values were determined from the total and GSSG concentration.

Determination of protein concentration

Total protein concentration was measured according to the method of Lowry, using bovine serum albumin as the standard (35).

Statistical analysis

Data were analyzed using Sigma Plot version 11.0 software (Systat Software Inc, USA). Data are presented as mean ± SD, and groups were compared using the Student's *t* test. Simple linear regression analysis (Pearson correlation coefficient) was used to test associations between continuous variables. P<0.05 was considered to be statistically significant.

RESULTS

HR, IS and mortality

The mean HR was not signficantly different between sham and infarcted groups (246±11 beats/min versus 222±22 beats/min). IS, measured using echocardiography, was 46.91±8.55%.

Cardiac function

Systolic function: LVEF and LVFS were decreased, while systolic diameter was enhanced in the infarcted group compared with sham animals (Table 1). An increase in the chamber diameter and loss of LV anterior wall contractility is also evident in Figure 1B. CO was not significantly different between the two groups (Table 1).

Diastolic function: E was not different between groups, but A was lower in the infarcted group (P=0.0038) compared with the control group (Figure 2B), resulting in an increase in the E/A ratio in the infarcted group (P=0.0048) (Table 1).

MPI: MPI was increased in the infarcted group (P=0.0009) compared with the control group (Table 1). A negative correlation between MPI and LVEF was also observed (r=−0.7019; P=0.035).

Oxidative damage and H_2O_2 concentration

Levels of lipid peroxidation and proteins carbonyls were not different between the two groups (Table 2). The H_2O_2 concentration was lower in the infarcted group compared with the sham group (P=0.040) (Figure 3A). A significant positive correlation between the concentration of H_2O_2 and LVEF was also observed (r=0.7723; P=0.0088).

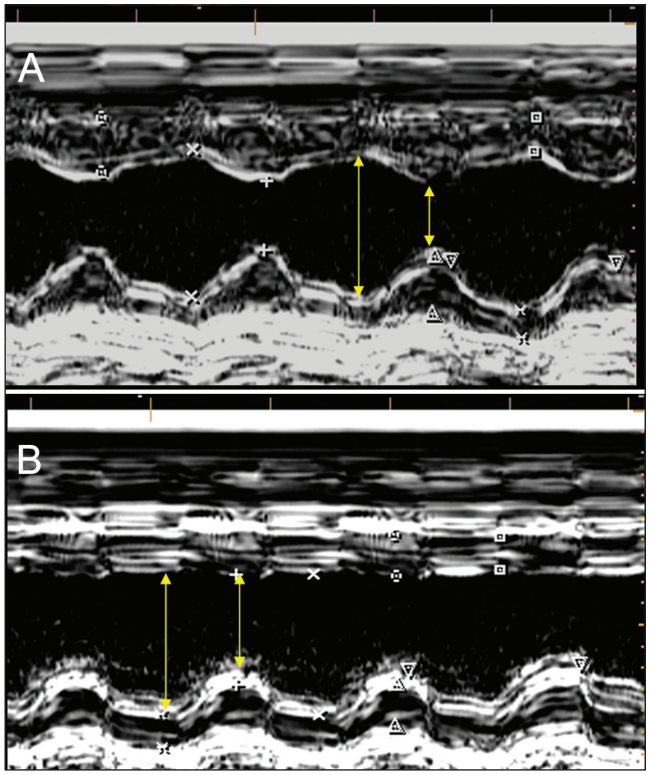

Figure 1) *An illustrative example of an M mode echocardiogram image of the left ventricle (LV) before (***A***) and after (***B***) myocardial infarction. Note the increase in the LV cavity and loss of LV free wall contractility*

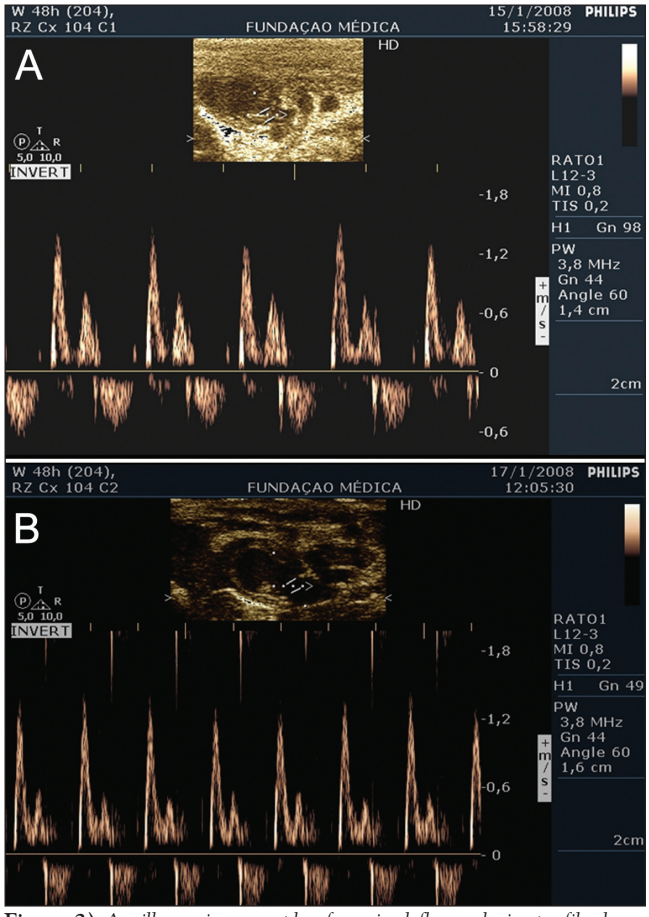

Figure 2) *An illustrative example of a mitral flow velocity profile determined by pulsed-wave Doppler before (***A***) and after (***B***) myocardial infarction. Note the decreased A wave after myocardial infarction in* **B**

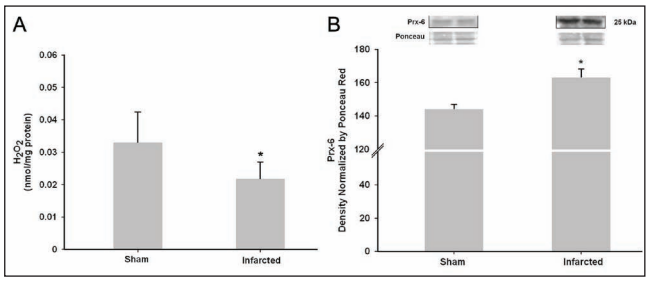

Figure 3) A *H_2O_2 concentration in heart homogenates from sham and infarcted groups. Data were analyzed using the Student's* t *test; P<0.05 was considered to be statistically significant.* **B** *Western blot analysis of peroxiredoxin-6 (Prx-6) in heart homogenates from sham and infarcted groups. Data presented as mean ± SD from four animals in each group (one representative gel of three Western blot experiments, showing two bands for each experimental group). Data were analyzed using the Student's* t *test; P<0.05 was considered to be statistically significant*

Antioxidant enzymes activities and expression

SOD and CAT activities did not differ between the two groups (Table 2). GPx activity was decreased by approximately 54% in the infarcted compared with the sham group (P=0.004). A significant positive correlation between GPx activity and LVEF was observed (r=0.67; P=0.0332). Conversely, Prx-6 protein expression was increased in the infarcted group compared with the sham group (P=0.0003) (Figure 3B).

GSH/GSSG ratio

The redox ratio (GSH/GSSG) was diminished by approximately 49% (P=0.02) in the infarcted group compared with the sham group (Table 2). A significant positive correlation between GSH/GSSG and LVEF was observed (r=0.78; P=0.02).

DISCUSSION

In the present study, we found that cardiac function was depressed at 48 h post-MI, as demonstrated by reduced LVEF and LVFS with preserved CO. Systolic dysfunction was also evident by an increase in systolic diameter, E/A ratio and MPI. Levels of oxidative damage to lipids and proteins remained unaltered at this early time point. Furthermore, myocardial H_2O_2 concentration and GPx activity were diminished, while Prx-6 protein levels were higher and the antioxidant activities of SOD and CAT were preserved.

Although cardiac remodelling subsequent to an ischemic insult has been previously studied in a rat model of MI, to date, there have been no studies that have assessed systolic and diastolic function in correlation to oxidative stress at such an early time point. Previous studies in the literature have focused on later time points after MI, when hallmarks of heart failure are already present (36). Therapeutic interventions at these time points may not always result in favourable functional recovery (37). Thus, our aim was to explore an earlier window of post-MI cardiac remodelling to better understand the biochemical changes related to oxidative stress that may be associated with the progression to heart failure.

A significant reduction in LVEF was evident as early as 48 h post-MI. LVFS was also decreased, thereby further confirming an impairment of ventricular contractility associated with LV chamber enlargement, as was evident by the enhanced systolic diameter. The data also demonstrated a loss of systolic function in the infarcted group at this time point. Additionally, it was observed that, although E was unchanged, A was depressed, resulting in an increase in the E/A ratio. The reduction in the slow filling phase appears to be associated with the increased residual fraction owing to the impaired LV contractility rather than to the loss of ventricular compliance, because diastolic diameter was not altered. Moreover, MPI, which reflects global LV function, was found to be markedly increased in the infarcted group.

TABLE 2
Oxidative stress parameters measured in heart homogenates from sham and infarcted groups

Variable	Group		P
	Sham	Infarcted	
LPO, cps/mg protein	5526±1228	6354±986	ns
Carbonyl, nmol/mg protein	2.12±0.55	1.82±0.31	ns
H_2O_2, nmol/mg protein	0.033±0.009	0.022±0.005	0.04
GSH/GSSG ratio	13.98±3.53	6.90±2.82	0.02
SOD activity, U/mg protein	5.76±2.3	4.80±1.9	ns
CAT activity, µmol/mg protein	37.76±6.8	34.06±9.9	ns
GPx, nmol/mg protein	47.83±10.1	25.60±7.97	0.004

Data expressed as mean ± SD; P values were calculated using Student's t *test. CAT Catalase; GPx Glutathione peroxidase; GSH Reduced glutathione; GSSG Oxidized glutathione; LPO Lipoperoxides; ns Not statistically significant; SOD Superoxide dismutase*

An increase in this index suggests an adaptive response of the heart in an attempt to maintain its pumping ability. In fact, CO was not changed at this time point, probably at the expense of an increased effort, indicating that, despite the loss of systolic function, the heart is still in a compensated stage.

With regard to oxidative stress markers, we did not find an increase in myocardial lipid peroxidation or protein oxidation at 48 h post-MI. Other studies have reported an increase in these markers at later time points, which was associated with ventricular dysfunction and heart failure (38,39). Interestingly, myocardial H_2O_2 concentrations were diminished at 48 h post-MI in our study, suggesting that these findings may represent countervailing survival mechanisms to maintain low H_2O_2 concentrations in this temporal window following MI. Prx enzymes function as H_2O_2 sensors because they contain cysteine residues susceptible to oxidation by ROS (40). These enzymes are located in different cellular compartments (15). Prx-6 is mainly localized to the cytosol and has been suggested to play a key role in ischemic injury (41). In our study, we observed that at an early time point, Prx-6 protein levels were significantly increased in the infarcted group compared with the sham group, which may have contributed to maintaining low H_2O_2 levels. During the process of peroxide detoxification, cysteine residues in the Prx-6 active site are reduced by GSH, which acts as an electron donor (15). This may have contributed to the reduced GSH/GSSG ratio found in our study, possibly due to the depletion of GSH in cardiac tissue. A decrease in the redox ratio also correlated with reduced LVEF in our study. Hill and Singal (4) have also reported that a decrease in the redox ratio at 16 weeks post-MI contributes to the development of heart failure. GSH is an important substrate for many enzymes involved in peroxide detoxification, including GPx. In fact, in the present study, we also observed a decrease in GPx activity. Furthermore, we found a positive correlation between GPx and LVEF, suggesting a strong association between cardiac function and the activity of this enzyme. These data also corroborate previous findings demonstrating that GPx overexpression inhibits the development of LV remodelling and failure after MI, which may contribute to improved survival (42) and the attenuation of diastolic dysfunction, myocyte hypertrophy and interstitial fibrosis (43). The other enzymatic antioxidants, SOD and CAT, were not altered at this early time point, suggesting that Prx is the major antioxidant that plays a role in maintaining low H_2O_2 levels. H_2O_2 acts as an important signalling molecule, whereby low concentrations of H_2O_2 are a signal for the activation of prosurvival pathways, while increased concentrations of H_2O_2 lead to proapoptotic signalling, as our group has previously demonstrated (39). Brixius et al (16) demonstrated that in the failing human myocardium, Prx-6 was the most altered isoform, demonstrated by a significant reduction in its expression. The downregulation of this enzyme was associated with heart failure, confirming its utility as a marker for this stage of cardiac dysfunction.

SUMMARY

Our data indicate that MI induced redox imbalances (reduced GSH/GSSG ratio) after 48 h, probably reflecting GSH consumption because it acts as a substrate for the antioxidant systems, thereby acting to maintain low concentrations of H_2O_2. This antioxidant adaptation results in lower oxidative damage to lipids and proteins and compensated cardiac function at 48 h post-MI. Overall, our results suggest that redox balance preservation by means of GSH recovery would be an important strategy to avoid the progression from the compensated to the decompensated stage and to improve ventricular remodelling after MI.

TECHNICAL SUPPORT: This research was supported by grants awarded by HCPA-FIPE (Research Support Fund) and CNPq (Brazilian Research Council).

REFERENCES

1. Davies KJ. Oxidative stress: The paradox of aerobic life. Biochem Soc Symp 1995;61:1-31.
2. Santos CX, Anilkumar N, Zhang M, Brewer AC, Shah AM. Redox signaling in cardiac myocytes. Free Radic Biol Med 2011;50:777-93.
3. Kutala VK, Khan M, Angelos MG, Kuppusamy P. Role of oxygen in postischemic myocardial injury. Antioxid Redox Signal 2007;9:1193-206.
4. Hill MF, Singal PK. Antioxidant and oxidative stress changes during heart failure subsequent to myocardial infarction in rats. Am J Pathol 1996;148:291-300.
5. Weber KT, Brilla CG. Pathological hypertrophy and cardiac interstitium. Fibrosis and renin-angiotensin-aldosterone system. Circulation 1991;83:1849-65.
6. Siwik DA, Tzortzis JD, Pimental DR, et al. Inhibition of copper-zinc superoxide dismutase induces cell growth, hypertrophic phenotype, and apoptosis in neonatal rat cardiac myocytes in vitro. Circ Res 1999;85:147-53.
7. Tsutsui H, Kinugawa S, Matsushima S. Oxidative stress and heart failure. Am J Physiol Heart Circ Physiol 2011;301:H2181-190.
8. Cai H. Hydrogen peroxide regulation of endothelial function: Origins, mechanisms, and consequences. Cardiovasc Res 2005;68:26-36.
9. Tsutsui H. Mitochondrial oxidative stress and heart failure. Intern Med 2006;45:809-13.
10. Aebi H. Catalase in vitro. Methods Enzymol 1984;105:121-6.
11. Sawyer DB, Siwik DA, Xiao L, Pimentel DR, Singh K, Colucci WS. Role of oxidative stress in myocardial hypertrophy and failure. J Mol Cell Cardiol 2002;34:379-88.
12. Fisher AB, Dodia C, Feinstein SI, Ho YS. Altered lung phospholipid metabolism in mice with targeted deletion of lysosomal-type phospholipase A2. J Lipid Res 2005;46:1248-56.
13. Trachootham D, Lu W, Ogasawara MA, Nilsa RD, Huang P. Redox regulation of cell survival. Antioxid Redox Signal 2008;10:1343-74.
14. Watson WH, Yang X, Choi YE, Jones DP, Kehrer JP. Thioredoxin and its role in toxicology. Toxicol Sci 2004;78:3-14.
15. Rhee SG, Woo HA, Kil IS, Bae SH. Peroxiredoxin functions as a peroxidase and a regulator and sensor of local peroxides. J Biol Chem 2012;287:4403-10.
16. Brixius K, Schwinger RH, Hoyer F, et al. Isoform-specific downregulation of peroxiredoxin in human failing myocardium. Life Sci 2007;81:823-31.
17. Pfeffer MA, Pfeffer JM, Fishbein MC, et al. Myocardial infarct size and ventricular function in rats. Circ Res 1979;44:503-12.
18. Tavares AM, da Rosa Araujo AS, Baldo G, et al. Bone marrow derived cells decrease inflammation but not oxidative stress in an experimental model of acute myocardial infarction. Life Sci 2010;87:699-06.
19. Nozawa E, Kanashiro RM, Murad N, et al. Performance of two-dimensional Doppler echocardiography for the assessment of infarct size and left ventricular function in rats. Braz J Med Biol Res 2006;39:687-95.
20. Peron AP, Saraiva RM, Antonio EL, Tucci PJ. Mechanical function is normal in remanent myocardium during the healing period of myocardial infarction despite congestive heart failure. Arq Bras Cardiol 2006;86:105-12.
21. Mercier JC, DiSessa TG, Jarmakani JM, et al. Two-dimensional echocardiographic assessment of left ventricular volumes and ejection fraction in children. Circulation 1982;65:962-9.
22. Litwin SE, Katz SE, Morgan JP, Douglas PS. Serial echocardiographic assessment of left ventricular geometry and function after large myocardial infarction in the rat. Circulation 1994;89:345-54.
23. Moises VA, Ferreira RL, Nozawa E, et al. Structural and functional characteristics of rat hearts with and without myocardial infarct. Initial experience with Doppler echocardiography. Arq Bras Cardiol 2000;75:125-36.
24. Cury AF, Bonilha A, Saraiva R, et al. Myocardial performance index in female rats with myocardial infarction: Relationship with ventricular function parameters by Doppler echocardiography. J Am Soc Echocardiogr 2005;18:454-60.
25. Llesuy SF, Milei J, Molina H, Boveris A, Milei S. Comparison of lipid peroxidation and myocardial damage induced by adriamycin and 4'-epiadriamycin in mice. Tumori 1985;71:241-9.
26. Gonzalez FB, Llesuy S, Boveris A. Hydroperoxide-initiated chemiluminescence: An assay for oxidative stress in biopsies of heart, liver, and muscle. Free Radic Biol Med 1991;10:93-100.
27. Reznick AZ, Packer L. Oxidative damage to proteins: Spectrophotometric method for carbonyl assay. Methods Enzymol 1994;233:357-63.
28. Pick E, Keisari Y. A simple colorimetric method for the measurement of hydrogen peroxide produced by cells in culture. J Immunol Methods 1980;38:161-70.
29. Araujo AS, Ribeiro MF, Enzveiler A, et al. Myocardial antioxidant enzyme activities and concentration and glutathione metabolism in experimental hyperthyroidism. Mol Cell Endocrinol 2006;249:133-9.
30. Laemmli UK. Cleavage of structural proteins during the assembly of the head of bacteriophage T4. Nature 1970;227:680-5.
31. Klein D, Kern RM, Sokol RZ. A method for quantification and correction of proteins after transfer to immobilization membranes. Biochem Mol Biol Int 1995;36:59-66.
32. Marklund SL. Superoxide dismutase isoenzymes in tissues and plasma from New Zealand black mice, nude mice and normal BALB/c mice. Mutat Res 1985;148:129-34.
33. Flohe L, Gunzler WA. Assays of glutathione peroxidase. Methods Enzymol 1984;105:114-21.
34. Anderson ME. Determination of glutathione and glutathione disulfide in biological samples. Methods Enzymol 1985;13:548-55.
35. Lowry OH, Rosebrough NJ, Farral AL, Randall RJ. Protein measurement with the Folin phenol reagent. J Biol Chem 1951;193:265-75.
36. Pinho CA, Tromm CB, Tavares AM, et al. Effects of different physical training protocols on ventricular oxidative stress parameters in infarction-induced rats. Life Sci 2012;90:553-9.
37. Ryder M, Beattie JM, O'Hanlon R, McDonald K. Multidsciplinary heart failure management and end of life care. Curr Opin Support Palliat Care 2011;5:317-21.
38. Hagen MK, Lehenbauer-Ludke AR, Paludo AC et al. Diet with isolated soy protein reduces oxidative stress and preserves ventricular function in rats with myocardial infarction. Nutr Metab Cardiovasc Dis 2009;19:91-7.
39. Schenkel PC, Tavares AMV, Fernandes RO, et al. Time course of hydrogen peroxide/thioredoxin balance and its influence on the intracellular signaling in myocardial infarction. Exp Physiol 2012;97:741-9.
40. Rhee SG, Woo HA. Multiple functions of peroxiredoxins: Peroxidases, sensors and regulators of the intracellular messenger H_2O_2, and protein chaperones. Antioxid Redox Signal 2011;15:781-94.
41. Godoy JR, Oesteritz S, Hanschmann EM, Ockenga W, Ackermann W, Lillig CH. Segment-specific overexpression of redoxins after renal ischemia and reperfusion: Protective roles of glutaredoxin 2, peroxiredoxin 3, and peroxiredoxin 6. Free Radic Biol Med 2011;51:552-61.
42. Shiomi T, Tsutsui H, Matsusaka H, et al. Overexpression of glutathione peroxidase prevents left ventricular remodeling and failure after myocardial infarction in mice. Circulation 2004;109:544-9.
43. Matsushima S, Kinugawa S, Ide T, et al. Overexpression of glutathione peroxidase attenuates myocardial remodeling and preserves diastolic function in diabetic heart. Am J Physiol Heart Circ Physiol 2006;291:H2237-245.